
Adaptive Deadline and Batch Layered Synchronized Federated Learning

Asaf Goren

Technion

asaf.goren@campus.technion.ac.il

Natalie Lang

Ben-Gurion University

langn@post.bgu.ac.il

Nir Shlezinger

Ben-Gurion University

nirshlezinger1@gmail.com

Alejandro Cohen

Technion

alecohen@technion.ac.il

Abstract

Federated learning (FL) enables collaborative model training across distributed edge devices while preserving data privacy, and typically operates in a round-based synchronous manner. However, synchronous FL suffers from latency bottlenecks due to device heterogeneity, where slower clients (stragglers) delay or degrade global updates. Prior solutions, such as fixed deadlines, client selection, and layer-wise partial aggregation, alleviate the effect of stragglers, but treat round timing and local workload as static parameters, limiting their effectiveness under strict time constraints. We propose **ADEL-FL**, a novel framework that jointly optimizes per-round deadlines and user-specific batch sizes for layer-wise aggregation. Our approach formulates a constrained optimization problem minimizing the expected ℓ_2 distance to the global optimum under total training time and global rounds. We provide a convergence analysis under exponential compute models and prove that ADEL-FL yields unbiased updates with bounded variance. Extensive experiments demonstrate that ADEL-FL outperforms alternative methods in both convergence rate and final accuracy under heterogeneous conditions.

1 Introduction

Federated learning (FL) is a decentralized machine learning paradigm where multiple clients collaboratively train a shared model under the coordination of a central server, without exchanging their raw data [1]. This approach enables learning from widespread data while preserving privacy and reducing communication by only transmitting model updates. FL has opened opportunities to leverage data from edge devices (smartphones, IoT, etc.) for tasks like text prediction and personalized models, all while keeping sensitive information local [2, 3].

Empirical distributed learning studies showed that some workers are often $5\times$ slower than the median worker under typical conditions [4]. In synchronous FL (as in the standard federated averaging (FedAvg) protocol [1]), the server must wait for all (or most) clients to send updates before proceeding, so a slow client (called a *straggler*) can become a bottleneck. This variability in device speed and availability leads to significant latency and can degrade the model if certain clients rarely contribute due to repeated timeouts.

Related Work A variety of approaches have been proposed to mitigate straggler impact in distributed learning and FL. A simple yet common strategy in synchronous stochastic gradient descent (SGD) is to impose a per-round deadline: the server aggregates whatever updates have arrived by a cutoff time T and ignores late submissions [5]. This *drop-stragglers* approach has been shown to converge at the same asymptotic rate as full participation [6]. However, discarding stragglers outright can waste useful computation and potentially bias the learned model (since slower devices might consistently be left out). An alternative approach alters FL to be asynchronous, avoiding waiting

for stragglers by incorporating each update as it arrives, at the cost of some updates being stale [7]. To reduce the impact of stale updates, staleness-aware aggregation methods were proposed, such as buffering or reweighting updates based on arrival time [8].

Several works aimed at alleviating the harmful effect of stragglers without sacrificing their contributions. Client selection protocols were proposed in [9] to account for expected latency, while potentially reducing the effective data coverage per round. Other methods allow variable workload or model size on different devices by, e.g., training smaller local models on weaker devices [10]. Recently, more refined strategies have leveraged the structure of deep networks by allowing partial model updates. Notably, straggler-aware layer-wise federated learning (SALF) [11] introduced layer-wise aggregation, where even slow clients contribute gradients for the layers they complete within the deadline. While this improves utilization and convergence, existing methods like SALF typically fix deadlines and batch sizes, missing the potential benefits of dynamically allocating both per-round time and per-client workload based on system heterogeneity.

Research Gap While prior work addresses straggler mitigation either at the round level (deadlines, client selection) or the local optimization level (layer-wise partial updates), there is no unified approach that optimizes both the *deadline* and the *local optimization* to best use the total available time. Yet these decisions are inherently coupled: longer deadlines enable more computation from stragglers, while local optimization procedure affects how much local data each client processes and how long each round takes. Furthermore, existing methods such as SALF default to applying a full FedAvg update when no updates are available for a layer, a practice that can misalign the model under strict time constraints.

Proposed Approach – ADEL-FL We propose *Adaptive Deadline and Batch Layered Federated Learning* (ADEL-FL), a novel framework that jointly optimizes per-round deadlines and the mini-batch sizes used for local learning, combined with layer-wise aggregation. In contrast to existing methods, which either fix the deadline per round or treat it as a heuristic hyperparameter, ADEL-FL actively schedules a different deadline for *each round*, as part of a global optimization objective. Specifically, ADEL-FL formulates the deadline assignment and mini-batch sizing as a constrained optimization problem aimed at minimizing the expected distance to the optimal model under total training time and communication round constraints.

Summary of Contributions:

- We introduce ADEL-FL, the first FL method to jointly optimize round deadlines and batch sizes with layer-wise aggregation, balancing between reducing stochastic gradient variance and mitigating deadline-induced truncation variance leading to improved convergence under time constraints. Unlike prior methods, our approach accounts for iteration-varying deadlines and modified batch sizes, and it preserves layer parameters when no updates are received.
- By modeling per-layer computation time using a realistic exponential distribution, which enables analytical estimates of expected updates under deadline constraints and guiding optimal allocation of time and workload, we provide convergence guarantees for ADEL-FL. We rigorously show that its partial updates are unbiased with bounded variance, and analyze its effect on convergence of the learning procedure.
- We show experimentally that ADEL-FL achieves superior convergence and accuracy compared to existing straggler mitigation approaches under heterogeneous settings. For example, we show an improvement of over 19% in validation accuracy for MNIST [12] and over 4% in CIFAR-10 [13] over existing methods.

The rest of the paper is structured as follows: Section 2 presents the system model and the problem formulation; Section 3 details ADEL-FL algorithm and optimization solution; Section 4 provides experimental results; and Section 5 concludes the paper.

2 Preliminaries and Problem Formulation

In this section, we lay the foundation for deriving ADEL-FL. We begin with modeling synchronous FL in Section 2.1, after which we introduce the system heterogeneity model and discuss its impact on local computation latency in Section 2.2. We then formulate the tackled problem in Section 2.3.

2.1 Federated Learning

In FL [1], a central server trains a model with n parameters denoted $\mathbf{w} \in \mathbb{R}^n$, utilizing data stored at a group of U users indexed by $u \in \{1, \dots, U\}$. Unlike traditional centralized learning, their corresponding datasets— $\mathcal{D}_1, \mathcal{D}_2, \dots, \mathcal{D}_U$ —cannot be transferred to the server due to privacy or communication restrictions [14]. Letting $F_u(\mathbf{w})$ denote the empirical risk function of the u th user, FL aims to find the parameters \mathbf{w}_{opt} which minimize the averaged empirical risk across all users, i.e.,

$$\mathbf{w}_{\text{opt}} = \arg \min_{\mathbf{w}} \left\{ F(\mathbf{w}) \triangleq \frac{1}{U} \sum_{u=1}^U F_u(\mathbf{w}) \right\}, \quad (1)$$

where we further assumed, for simplicity, that the local datasets are all of the same cardinality.

Broadly speaking, FL follows an iterative procedure operated in rounds. In the t th round, the server transmits the current global model \mathbf{w}_t to the participating users, who each updates the model using its local dataset and computational resources. These updates are then broadcasted back to the server, which aggregates them to form the new global model; and this process continues until desired convergence is reached. In particular, conventional FL involves training at the devices via local-SGD [15] and server's aggregation using FedAvg [1]. The former takes the form

$$\mathbf{w}_{t+1}^u \leftarrow \mathbf{w}_t - \eta_t \nabla F_u(\mathbf{w}_t; i_t^u), \quad (2)$$

where i_t^u is the batch index chosen uniformly from all batches of cardinality S_u in \mathcal{D}_u , and η_t is the learning rate. For FedAvg, the aggregation rule is given by

$$\mathbf{w}_{t+1} \triangleq \frac{1}{U} \sum_{u=1}^U \mathbf{w}_{t+1}^u = \mathbf{w}_t - \eta_t \frac{1}{U} \sum_{u=1}^U \nabla F_u(\mathbf{w}_t; i_t^u). \quad (3)$$

Once (3) is employed for *synchronous* FL [1], the server has to ‘wait’ for the updates to arrive from all participating devices. This, in turn, can induce notable latencies and delays once the edge clients are highly computationally heterogeneous, as discussed next.

2.2 Computational Heterogeneity

In FL, participating edge devices often exhibit significant variability in their computational capabilities, resulting in different processing times for computing the local model updates (gradients) in (2) [4]. Formally, considering the u th user at global round t , let T_t^u be the computational time required for locally calculating its corresponding gradient $\nabla F_u(\mathbf{w}_t; i_t^u)$. The individual computational speed T_t^u can dramatically alter with respect to both u and t due to hardware limitations or additional computational tasks being executed concurrently. Consequently, the overall computational latency per round t in synchronous FL is determined by the *slowest* device, namely, $\max_u T_t^u$.

This constraint can make synchronous FL abortive for time-sensitive applications, where rapid learning is essential, as discussed in Section 1. This can be tackled, e.g., by imposing a global, per-round, fixed deadline T_t^d of maximum allowable computation time [5]. Accordingly, nodes not meeting the deadline termed *stragglers* are dropped in aggregation such that (3) transforms into

$$\mathbf{w}_{t+1}^{\text{drop}} = \mathbf{w}_t^{\text{drop}} - \eta_t \frac{1}{|\mathcal{U}_t|} \sum_{u \in \mathcal{U}_t} \nabla F_u(\mathbf{w}_t^{\text{drop}}; i_t^u), \quad \text{where } \mathcal{U}_t = \{u \mid T_t^u \leq T_t^d\}. \quad (4)$$

SALF [11] improves upon (4) by, instead of dropping the stragglers, utilizes their partial gradients that are calculated within the deadline limitation, forming the global model in a layer-wise fashion. In particular, for an L -layer neural network $\mathbf{w}_t = [\mathbf{w}_t^1, \dots, \mathbf{w}_t^L]^T$, (4) changes into updating each layer l separately via

$$\tilde{\mathbf{w}}_{t+1}^l = \begin{cases} \tilde{\mathbf{w}}_t^l, & \text{if } |\mathcal{U}_t^l| = 0, \quad \text{for } \mathcal{U}_t^l \subseteq \{1, \dots, U\} \\ \frac{1}{1-p_l} \left(\sum_{u \in \mathcal{U}_t^l} \frac{1}{|\mathcal{U}_t^l|} \tilde{\mathbf{w}}_{u,t}^l - p_l \tilde{\mathbf{w}}_t^l \right) & \text{otherwise, for } p_l \in \mathbb{R}, \end{cases} \quad (5)$$

where $p_l \triangleq P(|\mathcal{U}_t^l| = 0)$ is a bias correction constant.

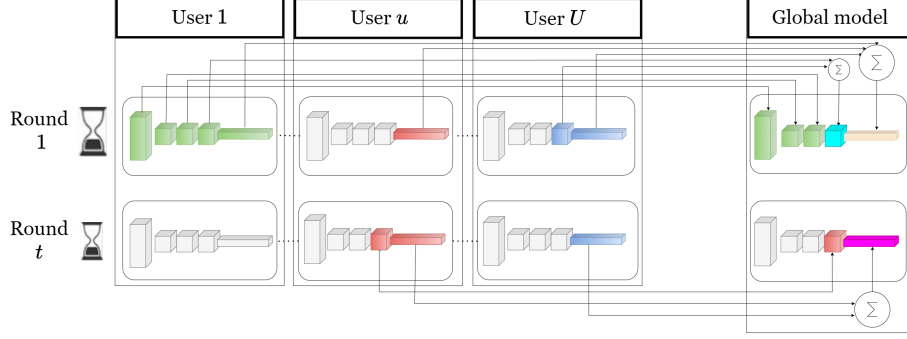


Figure 1: ADEL-FL illustration. Each user performs depth-limited backpropagation, with the extent of computation governed by the deadline. The server aggregates layer-wise gradients across users using only the layers received before the deadline. The color of each layer reflects the set of users that contributed to it, visualized by blending the corresponding user colors. For example, if User 1 is green and User U is blue, a cyan-colored layer indicates that both contributed to that layer in the current round.

2.3 Problem Formulation

For low-latency and dynamic heterogeneous FL setting, the timing limitation is often static, rather than varying per-round [16]. Additionally, the total number of global rounds is also commonly restricted, to limit the communication load [17]. Thus, we aim to enhance straggler-aware FL by meeting the following requirements:

- R1 Total rounds:* The FL procedure cannot surpass R global rounds.
- R2 Total training time:* The total time required for tuning of the FL model parameters is at most T_{\max} . That is, if the execution time of the t th FL round is T_t^d , then $\sum_{t=1}^R T_t^d \leq T_{\max}$.
- R3 Devices heterogeneity:* Users differ in their computational capabilities, which implies that the latency of computing the gradients for a data batch can greatly vary between users.

3 ADEL-FL

Evidently, Requirements *R1-R3* can be satisfied by setting $T_t^d = T_{\max}/R$, fixing the batch sizes, and employing layer-wise aggregation in (5). Nevertheless, the need to meet *R1-R3* while achieving a high-performance FL model learned in dynamically changing environments, motivates an optimized choice of T_t^d to best leverage the available local resources per round t . Moreover, as the local computation time of a user can be altered via its local training hyperparameters, and particularly its batch size, we seek a joint optimization of the per-round deadline and per-user batch size.

The proposed ADEL-FL scheme dynamically combines layer-wise aggregation as in (5) with varying deadline and local optimization, as illustrated in Figure 1. To derive how ADEL-FL sets its deadlines and mini-batch sizes, we first formulate a constrained optimization problem using the expected ℓ_2 distance. Next, in Section 3.2 we derive the bound on the ℓ_2 distance and in Section 3.3 we present the overall ADEL-FL algorithm.

3.1 Optimization Problem

Section (2.3) motivates formulating a constrained optimization problem holding *R1-R3*. To cope with *R3*, we allow the batch sizes to vary between users, drawing inspiration from previous works [18, 19] that advocated the usage of different batch sizes to deal with heterogeneity. Accordingly, we commence by determining a cost function that captures the model performance as a function of the deadlines $\{T_t^d\}_{t=1}^R$ and the local batch sizes $\{S_u\}_{u=1}^U$. To maintain a tractable analysis, we use a single parameter m to control the batch size across devices. Specifically, we introduce a parameter P_u for each user u , that is related to its computational capability, and set its batch size to be $S_u = \lceil m \cdot P_u \rceil$. This proportionality ensures that faster devices do not dominate training by contributing excessively more updates within the same deadline, which could bias the model toward their data and hinder convergence to the global optimum w_{opt} in (1).

Following the common practice in the FL literature [6, 20, 21], we assess the learned FL model via its expected ℓ_2 distance to the optimal FL model. Accordingly, by letting $\tilde{w}_t(\{T_\tau^d\}, m)$ denote the global model obtained at round t via layer-wise aggregation (5) with deadlines $\{T_\tau^d\}_{\tau \leq t}$ and

mini-batch sizes $\{S_u = \lceil m \cdot P_u \rceil\}_{u=1}^U$, we design ADEL-FL based on the following optimization framework:

Problem 1. For a total time budget T_{\max} and a fixed number of rounds R , minimize the expected squared distance between $\tilde{\mathbf{w}}_{R+1}$ and the global optimum \mathbf{w}_{opt} :

$$\min_{\{T_t^d\}_{t=1}^R, m} \mathbb{E} \left[\|\tilde{\mathbf{w}}_{R+1}(\{T_t^d\}_{t=1}^R, m) - \mathbf{w}_{\text{opt}}\|^2 \right] \quad \text{s.t.} \quad \sum_{t=1}^R T_t^d \leq T_{\max}.$$

3.2 Deriving the Cost Function

We now turn our attention to explicitly derive the cost function of Problem 1 for the layer-wise federated operation. The modified operation of ADEL-FL means that existing FL analyses for scenarios with partial device participation (such as the one found in [6]) do not directly hold here. Thus, to derive a concrete policy from Problem 1, we next lay out the assumptions that underpin our analysis, along with the statistical characteristics of the stragglers. Following this, we present the derivation of the convergence bound. All proofs are delegated to the appendix.

3.2.1 Assumptions

We perform the derivation of the cost function under the following assumptions, commonly adopted in FL studies [6, 22, 11, 23]:

A1 *Convexity and Smoothness*: The local objectives $\{F_u(\cdot)\}_{u=1}^U$ are ρ_c -strongly convex and ρ_s -smooth. That is, for all $\mathbf{w}_1, \mathbf{w}_2 \in \mathbb{R}^n$, it holds that

$$\begin{aligned} (\mathbf{w}_1 - \mathbf{w}_2)^T \nabla F_u(\mathbf{w}_2) + \frac{1}{2} \rho_c \|\mathbf{w}_1 - \mathbf{w}_2\|^2 &\leq F_u(\mathbf{w}_1) - F_u(\mathbf{w}_2) \leq \\ &(\mathbf{w}_1 - \mathbf{w}_2)^T \nabla F_u(\mathbf{w}_2) + \frac{1}{2} \rho_s \|\mathbf{w}_1 - \mathbf{w}_2\|^2. \end{aligned}$$

A2 *Variance Bound*: For each user u and round index t , the variance of the batch gradient $\nabla F_u(\mathbf{w}; i_t^u)$ is bounded by $\frac{\sigma_u^2}{S_u}$ for all $\mathbf{w} \in \mathbb{R}^n$, i.e.,

$$\mathbb{E} \left[\|\nabla F_u(\mathbf{w}; i_t^u) - \nabla F_u(\mathbf{w})\|^2 \right] \leq \frac{\sigma_u^2}{S_u}.$$

A3 *Gradient Bound*: For each user u and round index t , the expected squared ℓ_2 norm of the stochastic gradients $\nabla F_u(\mathbf{w}; i_t^u)$ is uniformly bounded by some G^2 for all $\mathbf{w} \in \mathbb{R}^n$, i.e.,

$$\mathbb{E} \left[\|\nabla F_u(\mathbf{w}; i_t^u)\|^2 \right] \leq G^2.$$

A4 *Computational Model*: Let $T_{t,u}^{b,l}$ be the computation time of user u in round t for the backpropagation of layer l . The random variables $\{T_{t,u}^{b,l}\}$ are i.i.d (in u , t , and l) and obey an exponential distribution:

$$T_{t,u}^{b,l} \sim \text{Exp} \left(\frac{S_u}{P_u} \right).$$

Under assumption A2, the variance of the batch gradient is inversely proportional to the batch size, referring to sampling with replacement of the samples. This relation is crucial in FL scenarios, as it directly links the user-level batch size to stability and convergence guarantees. Such variance-batch proportionality is supported in prior works (e.g., [15], [6]). Assumption A4 models the computation time of a layer as an exponential random variable. The exponential model is memoryless and well-suited for modeling compute time variability in deadline-constrained execution. This assumption aligns with prior work in straggler modeling and distributed training analysis [24, 25, 26], where exponential or shifted-exponential distributions are used to enable tractable performance bounds and scheduling policies. In addition, we define the heterogeneity gap, quantifying the differences in data distribution between users [6]:

$$\Gamma \triangleq F(\mathbf{w}_{\text{opt}}) - \frac{1}{U} \sum_{u=1}^U \min_{\mathbf{w}} F_u(\mathbf{w}),$$

where \mathbf{w}_{opt} is defined in (1).

3.2.2 Convergence Bound

After presenting the assumptions, we can now derive the bias correction factor p_l defined in (5):

Lemma 1. *When Assumptions A1-A4 hold, the value of $p_l \triangleq P(|\mathcal{U}_t^l| = 0)$ is given by:*

$$p_l = Q\left(L + 1 - l, \frac{T_t^d}{m}\right)^U,$$

where $Q(s, x) \triangleq \frac{1}{\Gamma(s)} \int_x^\infty t^{s-1} e^{-t} dt$ is the regularized upper incomplete gamma function [27].

As expected, p_l is monotonically decreasing with the layer index l , as the recursive structure of the backpropagation algorithm implies that first layers are less likely to be reached under tight deadline. Using Lemma 1, we state two lemmas for unbiasedness and bounded variance of each round of our proposed framework:

Lemma 2. *(Unbiasedness). Under Assumptions A1-A4, for every FL round of index t , the global model aggregated via ADEL-FL using (5) is an unbiased estimator of the one obtained via vanilla FedAvg [6], namely,*

$$\mathbb{E}[\tilde{\mathbf{w}}_{t+1}^l] = \mathbf{w}_{t+1}^l,$$

where \mathbf{w}_{t+1}^l is given by (3).

Lemma 3. *(Bounded variance) Consider ADEL-FL with Assumptions A1-A4 and the learning rate η_t set to be non-increasing and satisfying $\eta_t \leq 2\eta_{t+1}$ and $p_1 < 0.5$. Then, for every FL round t , the expected difference between $\tilde{\mathbf{w}}_{t+1}$ and \mathbf{w}_{t+1} , which is the variance of $\tilde{\mathbf{w}}_{t+1}$, is bounded by:*

$$\mathbb{E}[\|\tilde{\mathbf{w}}_{t+1} - \mathbf{w}_{t+1}\|^2] \leq \eta_t^2 G^2 \frac{4U}{(U-1)} \sum_{l=1}^L \frac{1 + Q\left(L + 1 - l, \frac{T_t^d}{m}\right)^U}{1 - 2Q\left(L + 1 - l, \frac{T_t^d}{m}\right)^U}.$$

Lemmas 2 and 3 are critical for establishing the convergence bound. Lemma 2 ensures that ADEL-FL update remains an unbiased estimator of the FedAvg update, preserving convergence direction. Lemma 3 guarantees that the variance introduced by partial updates remains controlled. These properties mirror the core assumptions required in classical FL convergence analyses, such as those in [6], and are necessary to derive a meaningful upper bound on the expected distance to \mathbf{w}_{opt} .

We are now ready to state the main theoretical result of this work: the cost function of Problem 1, which is the convergence bound for the ADEL-FL algorithm under Assumptions A1-A4. This result characterizes how the joint selection of training deadlines and batch size scaling affects the convergence behavior, accounting for both user heterogeneity and partial gradient contributions.

Theorem 1. *Consider ADEL-FL with Assumptions A1-A4, where the learning rate η_t is set to be non-increasing and holds $\eta_t \leq 2\eta_{t+1}$ and $\eta_1 \leq \frac{1}{4\rho_s}$. Then, we have:*

$$\mathbb{E}[\|\tilde{\mathbf{w}}_{R+1} - \mathbf{w}_{\text{opt}}\|^2] \leq \prod_{t=1}^R (1 - \eta_t \rho_c) \Delta_1 + \sum_{t=1}^R \eta_t^2 (B + C_t) \prod_{\tau=t+1}^R (1 - \eta_\tau \rho_c),$$

where $\Delta_1 \triangleq \mathbb{E}[\|\tilde{\mathbf{w}}_1 - \mathbf{w}_{\text{opt}}\|^2]$, and B and C_t are given by:

$$B \triangleq \frac{1}{mU^2} \sum_{u=1}^U \frac{\sigma_u^2}{P_u} + 6\rho_s \Gamma \quad C_t \triangleq G^2 \frac{4U}{U-1} \sum_{l=1}^L \frac{1 + Q\left(L + 1 - l, \frac{T_t^d}{m}\right)^U}{1 - 2Q\left(L + 1 - l, \frac{T_t^d}{m}\right)^U}.$$

The convergence bound depends on the constants B and C_t , which capture a trade-off between SGD variance reduction and deadline-induced truncation. This trade-off is analyzed in detail in Section 3.4.

3.3 ADEL-FL Algorithm

Having derived the cost function in Theorem 1, we now formulate the full optimization problem, which jointly determines the round-wise deadlines $\{T_t^d\}_{t=1}^R$ and the global batch-scaling parameter m based on Problem 1. This optimization reflects the practical trade-off between computation progress and user participation in time-limited heterogeneous federated environments.

Problem 2. Given the convergence bound in Theorem 1, minimize the upper bound on the expected squared ℓ_2 distance between $\tilde{\mathbf{w}}_{R+1}$ and the global optimum \mathbf{w}_{opt} under a total time budget T_{max} :

$$\min_{\{T_t\}_{t=1}^R, m} \prod_{t=1}^R (1 - \eta_t \rho_c) \Delta_1 + \sum_{t=1}^R \eta_t^2 (B + C_t) \prod_{\tau=t+1}^R (1 - \eta_\tau \rho_c) \quad \text{s.t.} \quad \sum_{t=1}^R T_t^d \leq T_{\text{max}}.$$

We solve Problem 2 using a trust-region method [28], an iterative strategy well-suited for nonconvex constrained optimization. Trust-region approaches approximate the objective by a local quadratic model and restrict updates to a neighborhood where the model is deemed reliable. The region's size is adaptively adjusted based on how well the approximation predicts true improvement. The optimization yields both the per-round deadlines and the batch-scaling factor. These are then embedded into the ADEL-FL procedure, summarized as Algorithm 1. Initially (Steps 1-3), the server solves the global optimization problem to allocate per-round deadlines T_t^d and computes each user's batch size $S_u = \lceil m \cdot P_u \rceil$ proportional to their computational capability. In each round t , users perform local training within their time limit (Steps 5-7), computing gradients up to a layer d_t^u based on how far they progress before the deadline, and then transmit those partial updates to the server. The server aggregates received gradients in a layer-wise manner (Steps 8-11), forming the global model update via the rule (5) while preserving the last available state when no updates arrive for a layer. This procedure repeats for R rounds, and the final model is returned in Step 14.

Algorithm 1 ADEL-FL

- 1: **Input:** Number of rounds R , training deadline T_{max} , learning rates $\{\eta_t\}_{t=1}^R$, computational capabilities $\{P_u\}_{u=1}^U$ and initial model \mathbf{w}_0
 - 2: Solve Problem 2 to find $\{T_t^d\}_{t=1}^R, m$
 - 3: Define batch sizes $S_u = \lceil m \cdot P_u \rceil$ for each $u \in \{1, \dots, U\}$
 - 4: **for** $t = 1, \dots, R$ **do**
 - 5: Clients Side - do in parallel for each u , until deadline T_t^d :
 - 6: Compute $\nabla F_u(\mathbf{w}_t, i_t^u)$ up to layer d_t^u
 - 7: Convey partial gradients to server
 - 8: Server Side - do after deadline time T_t^d :
 - 9: **for** $l = 1, \dots, L$ **do**
 - 10: Recover the participating user set \mathcal{U}_t^l
 - 11: Compute $\tilde{\mathbf{w}}_{t+1}^l$ via Equation (5)
 - 12: **end for**
 - 13: **end for**
 - 14: **Output:** Trained model \mathbf{w}_{R+1}
-

The overall strategy of ADEL-FL refines the convergence guarantees derived earlier by optimally tuning the time-budgeted training configuration. By solving Problem 2, we adaptively allocate deadlines and batch sizes to each round, enabling balanced participation and efficient learning. The resulting algorithm demonstrates improved performance under strict time constraints, as empirically demonstrated in Section 4.

3.4 Discussion

The cost function in Problem 2 reflects a fundamental trade-off between the terms B and C_t , which capture distinct sources of error. The term $B = \frac{1}{mU^2} \sum_{u=1}^U \frac{\sigma_u^2}{P_u} + 6\rho_s\Gamma$ corresponds to the variance induced by stochastic gradients, and is inversely proportional to the global batch scaling factor m . Thus, increasing m (i.e., using larger batches) reduces B , reducing the user's SGD variance. However, larger batches require more computation per user, potentially reducing the number of clients able to contribute full updates within a fixed deadline. This effect is captured by C_t , which quantifies the variance due to partial participation and depends on the regularized incomplete gamma function. As m increases, C_t worsens due to fewer layers being computed per user under time constraints as in Requirement R2. In addition, the per-round deadline T_t^d must be judiciously allocated across rounds to align with the learning rate schedule and batch size configuration, ensuring that each round maximally leverages the available computational budget while preserving convergence efficiency.

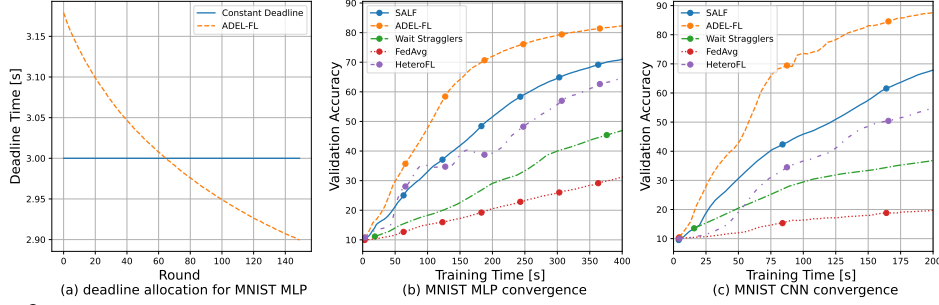


Figure 2: Deadline allocation and convergence curves for MNIST using an inverse decaying learning rate. (a) Adaptive deadline per round for ADEL-FL (MLP). (b) Convergence (validation accuracy vs. training time), MLP. (c) Convergence, CNN.

A natural extension of ADEL-FL is to also optimize the number of rounds R , in addition to T_t^d and m . In practical deployments, both the number of rounds and the overall latency are often constrained. Optimizing over R introduces an additional degree of flexibility, allowing the system to determine the optimal number of global rounds given the available time budget. This joint optimization problem—over the number of rounds R , per-round deadlines $\{T_t^d\}$, and batch scaling m —could be formulated as a mixed-integer constrained program or tackled with adaptive scheduling heuristics, replacing Problem 2 in line 2 of the algorithm. Incorporating this optimization into ADEL-FL would further enhance its applicability to time-critical FL scenarios.

4 Experimental Results

We empirically evaluate ADEL-FL for training image classification models using MNIST [12] and CIFAR-10 [13]. We consider a series of experiments of increasing complexity. In each case, we compare ADEL-FL against four baseline schemes: (i) *Wait Stragglers*: the standard federated averaging with full client participation (synchronous FedAvg with the server waiting for all devices each round) [1]; (ii) *Drop-Stragglers*: synchronous FedAvg with a fixed per-round deadline that drops any late client updates [5]; (iii) *SALF*: – the straggler-aware FL method suggested in [11], which aggregates partial gradients from slow devices but uses a fixed deadline and batch size; and (iv) *HeteroFL*, which trains local submodels with reduced width according to each client’s capability, allowing efficient aggregation into a full global model [10]. All methods are evaluated under a fixed total training time budget T_{\max} and a fixed number of communication rounds R (per the constraints in Requirements *R1–R2*). Experiments are conducted on a Linux server with NVIDIA A30 GPU. To emulate heterogeneous device speeds in a controlled manner, we sample each client’s computation time per layer from an exponential distribution (as in Assumption *A4*). We begin with image classification tasks on MNIST and CIFAR-10 using an inverse-decay learning rate schedule $\eta_t = \eta_0 / (1 + t)$ with initial $\eta_0 \in \{0.05, 0.1, 0.5, 1.0\}$ to assess baseline convergence behavior. Next, we analyze stability and optimization dynamics under constant learning rate and adding ℓ_2 regularization, deviating from the assumptions of Theorem 1. Finally, we present a comparative table summarizing performance across varying total training times, highlighting ADEL-FL’s efficiency under strict time constraints.

MNIST We first evaluate on the MNIST dataset [12] (handwritten 28×28 grayscale digits). The data are partitioned uniformly at random across $U = 20$ users (each client holds $1/20$ of the training set of 60,000 images). We choose the total training time T_{\max} and number of rounds R such that, under a standard local minibatch size, the average fraction of each model updated per round (i.e. the average backpropagation depth) is 50% of the network layers. We consider two model architectures of different capacity: (1) MLP: a simple fully-connected network with two hidden layers (32 and 16 neurons) and a softmax output; (2) CNN: a small CNN with two 5×5 convolutional layers (each followed by max-pooling and ReLU [29]) and two dense layers, ending in a softmax output.

Figure 2(a) shows that the traditional constant deadline allocation versus the proposed deadline allocation which decreases over time, similarly to the learning rate, optimizing early contributions from slower devices. Figure 2(b) and (c) demonstrates that ADEL-FL achieves faster and higher convergence than baselines while dynamically adapting deadlines to gradually accelerate training. ADEL-FL substantially outperforms *Drop-Stragglers*, *Wait Stragglers* and *HeteroFL*, which suffer from slow or stalled convergence. *SALF* mitigates stragglers but remains less efficient than ADEL-FL,

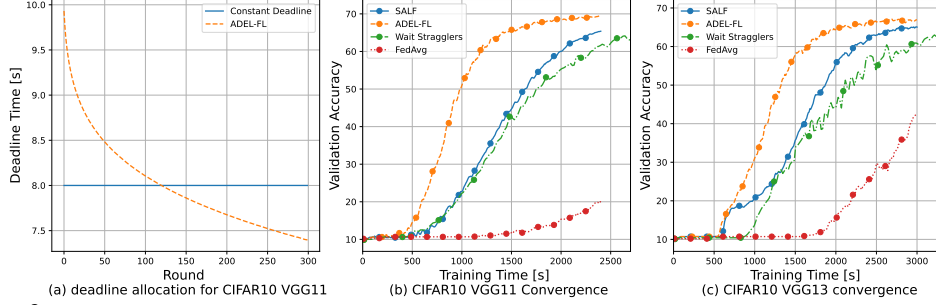


Figure 3: Deadline allocation and convergence curves for CIFAR10 using an inverse decaying learning rate. (a) Adaptive deadline per round for ADEL-FL (VGG11). (b) Convergence, VGG11. (c) Convergence, VGG13.

particularly in early training, where larger deadlines allow more layers to be updated. For example, ADEL-FL achieves over 20% accuracy improvement on MLP at time 180[s] compared to SALF.

CIFAR-10 Next, we evaluate on the CIFAR-10 simulating an FL system with $U = 30$ users, each receiving an equal partition of the 50,000 training images. In these experiments, we focus on deeper neural network models. We train two architectures of the VGG family [30]: VGG11 and VGG13, which have 8 and 10 convolutional layers (respectively) followed by 3 fully-connected layers. These networks are substantially deeper than the MNIST models, providing a more challenging and heterogeneous workload. We set the global time budget T_{\max} and rounds R such that the average local computation per round reaches about 85% of each model’s full depth for a baseline batch size – i.e., on average clients nearly complete a full pass through the network each round under the time limit. Results are shown in Figure 3. ADEL-FL consistently outperforms SALF, Drop-Stragglers, and Wait Stragglers, achieving faster convergence while maintaining a higher final accuracy (69% for ADEL-FL vs 65% for SALF). As in MNIST, the deadline allocation decreases over time alongside the decaying learning rate, efficiently balancing training speed and convergence.

Robustness to Learning Assumptions

To validate ADEL-FL under conditions where optimization assumptions are violated, we perform two studies on CIFAR-10 VGG11, reported in Figure 4. First, we introduce ℓ_2 regularization on local objectives. Second, we fix the learning rate $\eta_t = \eta_0$ instead of using a decaying profile. These modifications deviate from theoretical conditions assumed for convergence in Theorem 1. Nevertheless, ADEL-FL maintains advantages over SALF, Wait-Stragglers and Drop-Stragglers. The convergence remains stable and outperforms the other existing solutions compared, demonstrating that ADEL-FL’s design is robust even when the actual optimization dynamics differs moderately from the assumed model.

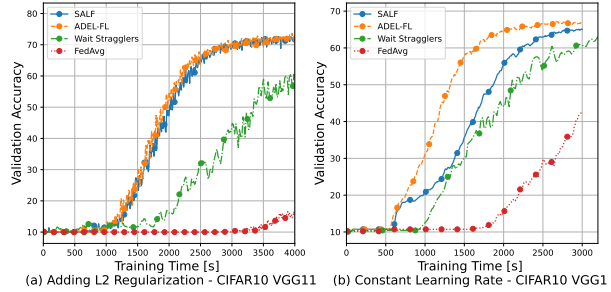


Figure 4: Robustness results, CIFAR-10 VGG11. (a) Convergence with ℓ_2 regularization. (b) Convergence with constant learning rate.

Training Time Table 1 compares final accuracy across different total training time budgets. Even under stringent time limits, ADEL-FL preserves superior convergence, highlighting its efficient use of limited computation. As the total training time T_{\max} increases, all methods generally benefit from improved model accuracy due to deeper local computations. However, ADEL-FL consistently maintains a noticeable gap over SALF, Wait-Stragglers and Drop-Stragglers across all budgets. In the low-budget regime, ADEL-FL is particularly advantageous, achieving much better performance while effectively handling the computation resources. In higher budget regimes, although the gap slightly narrows, ADEL-FL continues to converge faster and achieves superior final performance.

T_{\max} [s]	ADEL-FL	SALF	Drop-Stragglers	FedAvg
1200	61	36	14	30
1600	66	50	16	46
2000	68	61	17	57
2400	69	66	20	63

Table 1: Final test accuracy (%) of ADEL-FL and baseline methods on CIFAR-10 (VGG11) under varying total training time budgets T_{\max} .

5 Conclusion

We introduced ADEL-FL, a novel FL framework that jointly optimizes per-round deadlines and client-specific batch sizes under a global training time constraint. By integrating adaptive scheduling with layer-wise aggregation, ADEL-FL effectively mitigates stragglers while preserving statistical efficiency. Our theoretical analysis establishes that ADEL-FL yields unbiased updates with bounded variance under exponential latency models, and our optimization formulation captures the convergence trade-offs induced by time allocation and batch scaling. Empirical results on standard benchmarks demonstrate that ADEL-FL consistently outperforms existing methods in convergence rate and final accuracy under heterogeneous settings.

References

- [1] Brendan McMahan, Eider Moore, Daniel Ramage, Seth Hampson, and Blaise Agüera y Arcas. Communication-efficient learning of deep networks from decentralized data. In *Artificial intelligence and statistics*, pages 1273–1282. PMLR, 2017.
- [2] Jiehan Zhou, Shouhua Zhang, Qinghua Lu, Wenbin Dai, Min Chen, Xin Liu, Susanna Pirttikangas, Yang Shi, Weishan Zhang, and Enrique Herrera-Viedma. A survey on federated learning and its applications for accelerating industrial internet of things, 2021. URL <https://arxiv.org/abs/2104.10501>.
- [3] Sawsan Abdulrahman, Hanine Tout, Hakima Ould-Slimane, Azzam Mourad, Chamseddine Talhi, and Mohsen Guizani. A survey on federated learning: The journey from centralized to distributed on-site learning and beyond. *IEEE Internet of Things Journal*, 8(7):5476–5497, 2021.
- [4] Rashish Tandon, Qi Lei, Alexandros G Dimakis, and Nikos Karampatziakis. Gradient coding: Avoiding stragglers in distributed learning. In *International Conference on Machine Learning*, pages 3368–3376. PMLR, 2017.
- [5] Jianmin Chen, Xinghao Pan, Rajat Monga, Samy Bengio, and Rafal Jozefowicz. Revisiting distributed synchronous SGD. *arXiv preprint arXiv:1604.00981*, 2016.
- [6] Xiang Li, Kaixuan Huang, Wenhao Yang, Shusen Wang, and Zhihua Zhang. On the convergence of fedavg on non-iid data. *arXiv preprint arXiv:1907.02189*, 2019.
- [7] Cong Xie, Sanmi Koyejo, and Indranil Gupta. Asynchronous federated optimization, 2020. URL <https://arxiv.org/abs/1903.03934>.
- [8] John Nguyen, Kshitiz Malik, Hongyuan Zhan, Ashkan Yousefpour, Michael Rabbat, Mani Malek, and Dzmitry Huba. Federated learning with buffered asynchronous aggregation, 2022. URL <https://arxiv.org/abs/2106.06639>.
- [9] Takayuki Nishio and Ryo Yonetani. Client selection for federated learning with heterogeneous resources in mobile edge. In *ICC 2019-2019 IEEE international conference on communications (ICC)*, pages 1–7. IEEE, 2019.
- [10] Enmao Diao, Jie Ding, and Vahid Tarokh. HeteroFL: Computation and communication efficient federated learning for heterogeneous clients. *arXiv preprint arXiv:2010.01264*, 2020.
- [11] Natalie Lang, Alejandro Cohen, and Nir Shlezinger. Stragglers-aware low-latency synchronous federated learning via layer-wise model updates. *IEEE Transactions on Communications*, pages 1–1, 2024.
- [12] Li Deng. The MNIST database of handwritten digit images for machine learning research [best of the web]. *IEEE signal processing magazine*, 29(6):141–142, 2012.
- [13] Alex Krizhevsky, Geoffrey Hinton, et al. Learning multiple layers of features from tiny images. 2009. URL <https://www.cs.utoronto.ca/~kriz/learning-features-2009-TR.pdf>.
- [14] Tomer Gafni, Nir Shlezinger, Kobi Cohen, Yonina C Eldar, and H Vincent Poor. Federated learning: A signal processing perspective. *IEEE Signal Processing Magazine*, 39(3):14–41, 2022.

- [15] Sebastian U Stich. Local SGD converges fast and communicates little. In *International Conference on Learning Representations*, 2019.
- [16] Kaiju Li, Hao Wang, and Qinghua Zhang. FedTCR: Communication-efficient federated learning via taming computing resources. *Complex & Intelligent Systems*, 9(5):5199–5219, 2023.
- [17] Younghyun Park, Dong-Jun Han, Do-Yeon Kim, Jun Seo, and Jaekyun Moon. Few-round learning for federated learning. *Advances in Neural Information Processing Systems*, 34: 28612–28622, 2021.
- [18] Zhenguo Ma, Yang Xu, Hongli Xu, Zeyu Meng, Liusheng Huang, and Yinxing Xue. Adaptive batch size for federated learning in resource-constrained edge computing. *IEEE Transactions on Mobile Computing*, 22(1):37–53, 2023.
- [19] Weijie Liu, Xiaoxi Zhang, Jingpu Duan, Carlee Joe-Wong, Zhi Zhou, and Xu Chen. AdaCoOpt: Leverage the interplay of batch size and aggregation frequency for federated learning. In *IEEE/ACM International Symposium on Quality of Service (IWQoS)*, 2023.
- [20] Hongda Wu and Ping Wang. Fast-convergent federated learning with adaptive weighting, 2021. URL <https://arxiv.org/abs/2012.00661>.
- [21] Yann Fraboni, Richard Vidal, Laetitia Kamani, and Marco Lorenzi. A general theory for federated optimization with asynchronous and heterogeneous clients updates, 2022. URL <https://arxiv.org/abs/2206.10189>.
- [22] Sebastian U. Stich. Local SGD converges fast and communicates little, 2019. URL <https://arxiv.org/abs/1805.09767>.
- [23] Donald Gross, John F Shortle, James M Thompson, and Carl M Harris. *Fundamentals of queueing theory*, volume 627. John wiley & sons, 2011.
- [24] Sanghamitra Dutta, Gauri Joshi, Soumyadip Ghosh, Parijat Dube, and Priya Nagpurkar. Slow and stale gradients can win the race: Error-runtime trade-offs in distributed SGD. In *International conference on artificial intelligence and statistics*, pages 803–812. PMLR, 2018.
- [25] Wenqi Shi, Sheng Zhou, and Zhisheng Niu. Device scheduling with fast convergence for wireless federated learning. In *IEEE International Conference on Communications (ICC)*, 2020.
- [26] Kangwook Lee, Maximilian Lam, Ramtin Pedarsani, Dimitris Papailiopoulos, and Kannan Ramchandran. Speeding up distributed machine learning using codes. *IEEE Transactions on Information Theory*, 64(3):1514–1529, 2017.
- [27] NIST Digital Library of Mathematical Functions. Chapter 8. Gamma and Related Functions. <https://dlmf.nist.gov/8.2>, 2023. Release 1.1.9 of 2023-03-15.
- [28] Ya-xiang Yuan. A review of trust region algorithms for optimization. *ICM99: Proceedings of the Fourth International Congress on Industrial and Applied Mathematics*, 09 1999.
- [29] Xavier Glorot, Antoine Bordes, and Y. Bengio. Deep sparse rectifier neural networks. volume 15, 01 2010.
- [30] Karen Simonyan and Andrew Zisserman. Very deep convolutional networks for large-scale image recognition. *International Conference on Learning Representations (ICLR)*, 2015. URL <https://arxiv.org/abs/1409.1556>.

A Technical Appendices and Supplementary Material

A.1 Appendix A - Proof of Lemma 1

We start by defining d_t^u as the depth reached by the user u in the round t , up to the deadline T_t^d . When Assumption A4 holds, backpropagation can be modeled as sequential layer gradient computation with exponential service time. We get a Poisson process, where d_t^u is closely related to the number of layers processed:

$$d_t^u = L + 1 - \min\{z_t^u, L\}, \quad \text{where} \quad z_t^u \sim \text{Poiss}\left(\frac{T_t^d}{m}\right).$$

Recall that $p_l \triangleq P(|\mathcal{U}_t^l| = 0)$ denotes the probability that no user contributes an update for layer l at round t . We use the i.i.d (by u) property of Assumption A4 to write:

$$P(|\mathcal{U}_t^l| = 0) = \bigcap_{u=1}^U P(z_t^u \leq L - l) = \prod_{u=1}^U P(z_t^u \leq L - l) = (P(z_t^1 \leq L - l))^U.$$

The probability mass function (PMF) of $X \sim \text{Poiss}(\lambda)$ is given by:

$$P(X = k) = \frac{\lambda^k e^{-\lambda}}{k!}, \quad \text{for } k = 0, 1, 2, \dots$$

We denote $\lambda_t \triangleq \frac{T_t^d}{m}$ and get:

$$P(|\mathcal{U}_t^l| = 0) = (P(z_t^1 \leq L - l))^U = \left(\sum_{k=0}^{L-l} \frac{\lambda_t^k e^{-\lambda_t}}{k!} \right)^U. \quad (\text{A.1})$$

For integer $s > 1$, we perform integration by parts with the choices:

$$\begin{aligned} u &= \frac{t^{s-1}}{\Gamma(s)}, & dv &= e^{-t} dt, \\ du &= \frac{t^{s-2}}{\Gamma(s-1)} dt, & v &= -e^{-t}. \end{aligned}$$

Applying integration by parts, we have:

$$\begin{aligned} Q(s, x) &= \left[-\frac{t^{s-1} e^{-t}}{\Gamma(s)} \right]_{t=x}^{\infty} + \frac{1}{\Gamma(s-1)} \int_x^{\infty} t^{s-2} e^{-t} dt \\ &= \frac{x^{s-1} e^{-x}}{\Gamma(s)} + Q(s-1, x) \\ &= \frac{x^{s-1} e^{-x}}{(s-1)!} + Q(s-1, x). \end{aligned}$$

Unfolding the recursion with stop condition $Q(1, x) = e^{-x}$ yields:

$$Q(s, x) = \sum_{k=0}^{s-1} \frac{x^k e^{-x}}{k!}. \quad (\text{A.2})$$

Now, substituting Eq. (A.1) into Eq. (A.2), we get:

$$p_l = P(|\mathcal{U}_t^l| = 0) = Q\left(L + 1 - l, \frac{T_t^d}{m}\right)^U,$$

proving Lemma 1. □

A.2 Appendix B - Proof of Lemma 2

We aim to demonstrate that $\tilde{\mathbf{w}}_{t+1}$, as defined in Eq. (5), serves as an unbiased estimator of \mathbf{w}_{t+1} from Eq. (3). To achieve this, we analyze the expectation of the l -th subvectors of both expressions, leveraging the decomposition of the gradient into layers. Given the batches $\{i_u^t\}$, the only randomness in \mathbf{w}_{t+1}^l originates from \mathcal{U}_t^l . Instead of directly computing the expectation over \mathcal{U}_t^l , we use the law of total expectation:

$$\mathbb{E}[\tilde{\mathbf{w}}_{t+1}^l] = \mathbb{E}[\mathbb{E}[\tilde{\mathbf{w}}_{t+1}^l | |\mathcal{U}_t^l|]] = \sum_{K=0}^U P(|\mathcal{U}_t^l| = K) \mathbb{E}[\tilde{\mathbf{w}}_{t+1}^l | |\mathcal{U}_t^l| = K].$$

Substituting the probability of $|\mathcal{U}_t^l| = 0$, denoted as p_l , we get:

$$\mathbb{E}[\tilde{\mathbf{w}}_{t+1}^l] = p_l \tilde{\mathbf{w}}_t^l + \sum_{K=1}^U P(|\mathcal{U}_t^l| = K) \frac{1}{1 - p_l} \left(\frac{1}{K} \mathbb{E} \left[\sum_{u \in \mathcal{U}_t^l} \mathbf{w}_{u,t}^l \middle| |\mathcal{U}_t^l| = K \right] - p_l \tilde{\mathbf{w}}_t^l \right).$$

By Lemma 4 in [6], when users are uniformly sampled without replacement, FedAvg provides an unbiased estimate of full device participation. Hence, we can write:

$$\frac{1}{K} \mathbb{E} \left[\sum_{u \in \mathcal{U}_t^l} \mathbf{w}_{u,t}^l \middle| |\mathcal{U}_t^l| = K \right] = \frac{1}{K} K \sum_{u=1}^U \frac{1}{U} \mathbf{w}_{u,t}^l = \mathbf{w}_{t+1}^l. \quad (\text{A.3})$$

Substituting this into our expectation computation and simplifying using the summation of probabilities, we obtain:

$$\mathbb{E}[\tilde{\mathbf{w}}_{t+1}^l] = p_l \tilde{\mathbf{w}}_t^l + \frac{\mathbf{w}_{t+1}^l - p_l \tilde{\mathbf{w}}_t^l}{1 - p_l} \sum_{u=1}^U P(|\mathcal{U}_t^l| = K).$$

Using:

$$\sum_{u=1}^U P(|\mathcal{U}_t^l| = K) = 1 - P(|\mathcal{U}_t^l| = 0) = 1 - p_l,$$

we get:

$$\mathbb{E}[\tilde{\mathbf{w}}_{t+1}^l] = p_l \tilde{\mathbf{w}}_t^l + \mathbf{w}_{t+1}^l - p_l \tilde{\mathbf{w}}_t^l = \mathbf{w}_{t+1}^l.$$

Since this equality holds for every layer $l \in \{1, \dots, L\}$, and the global model $\tilde{\mathbf{w}}_{t+1}$ is formed by stacking the layer-wise vectors $\tilde{\mathbf{w}}_{t+1}^l$, it follows that the full model update is also unbiased:

$$\mathbb{E}[\tilde{\mathbf{w}}_{t+1}] = \mathbf{w}_{t+1},$$

completing the proof. \square

A.3 Appendix C - Proof of Lemma 3

For each layer l and round t , we define the variance of the layer update as $v_t^l \triangleq \mathbb{E}[\|\tilde{\mathbf{w}}_t^l - \mathbf{w}_t^l\|^2]$.

Using the law of total expectation with respect to the random variable $|\mathcal{U}_t^l|$:

$$\begin{aligned} v_{t+1}^l &\triangleq \mathbb{E}[\|\tilde{\mathbf{w}}_{t+1}^l - \mathbf{w}_{t+1}^l\|^2] = P(|\mathcal{U}_t^l| = 0) \mathbb{E}[\|\tilde{\mathbf{w}}_{t+1}^l - \mathbf{w}_{t+1}^l\|^2 | |\mathcal{U}_t^l| = 0] \\ &\quad + \sum_{K=1}^U P(|\mathcal{U}_t^l| = K) \mathbb{E}[\|\tilde{\mathbf{w}}_{t+1}^l - \mathbf{w}_{t+1}^l\|^2 | |\mathcal{U}_t^l| = K]. \end{aligned} \quad (\text{A.4})$$

For the first summoned, it holds that:

$$\begin{aligned}
\mathbb{E} \left[\|\tilde{\mathbf{w}}_{t+1}^l - \mathbf{w}_{t+1}^l\|^2 \mid |\mathcal{U}_t^l| = 0 \right] &= \mathbb{E} \left[\|\tilde{\mathbf{w}}_t^l - \mathbf{w}_{t+1}^l\|^2 \right] = \mathbb{E} \left[\|\tilde{\mathbf{w}}_t^l - \mathbf{w}_t^l + \mathbf{w}_t^l - \mathbf{w}_{t+1}^l\|^2 \right] \\
&\stackrel{(a)}{\leq} \mathbb{E} \left[\|\tilde{\mathbf{w}}_t^l - \mathbf{w}_t^l\|^2 \right] + \mathbb{E} \left[\|\mathbf{w}_{t+1}^l - \mathbf{w}_t^l\|^2 \right] \stackrel{(b)}{\leq} v_t^l + \sum_{u=1}^U \frac{1}{U} \mathbb{E} \left[\|\tilde{\mathbf{w}}_{u,t}^l - \mathbf{w}_t^l\|^2 \right] \\
&= v_t^l + \sum_{u=1}^U \frac{1}{U} \|\eta_t \nabla F_u(\mathbf{w}_t; i_t^u)\|^2 \stackrel{(c)}{\leq} v_t^l + \eta_t^2 G^2,
\end{aligned} \tag{A.5}$$

where (a) is given by the triangle inequality, (b) from the convexity of $\|\cdot\|^2$ and (c) from Assumption A3.

For the second summoned:

$$\begin{aligned}
\mathbb{E} \left[\|\tilde{\mathbf{w}}_{t+1}^l - \mathbf{w}_{t+1}^l\|^2 \mid |\mathcal{U}_t^l| = K \right] &= \mathbb{E} \left[\left\| \frac{1}{1-p_l} \left(\sum_{u \in \mathcal{U}_t^l} \frac{1}{|\mathcal{U}_t^l|} \mathbf{w}_{u,t}^l - p_l \tilde{\mathbf{w}}_t^l \right) - \mathbf{w}_{t+1}^l \right\|^2 \mid |\mathcal{U}_t^l| = K \right] \\
&= \frac{1}{(1-p_l)^2} \left(\mathbb{E} \left[\left\| \sum_{u \in \mathcal{U}_t^l} \frac{1}{|\mathcal{U}_t^l|} \mathbf{w}_{u,t}^l - \mathbf{w}_{t+1}^l - p_l (\tilde{\mathbf{w}}_t^l - \mathbf{w}_{t+1}^l) \right\|^2 \mid |\mathcal{U}_t^l| = K \right] \right) \\
&= \frac{1}{(1-p_l)^2} \times \\
&\left(\mathbb{E} \left[\left\| \sum_{u \in \mathcal{U}_t^l} \frac{1}{|\mathcal{U}_t^l|} \mathbf{w}_{u,t}^l - \mathbf{w}_{t+1}^l \right\|^2 \mid |\mathcal{U}_t^l| = K \right] \right)
\end{aligned} \tag{A.6}$$

$$+ p_l^2 \mathbb{E} \left[\|\tilde{\mathbf{w}}_t^l - \mathbf{w}_{t+1}^l\|^2 \right] \tag{A.7}$$

$$- 2p_l (\tilde{\mathbf{w}}_t^l - \mathbf{w}_{t+1}^l)^R \mathbb{E} \left[\left(\sum_{u \in \mathcal{U}_t^l} \frac{1}{|\mathcal{U}_t^l|} \mathbf{w}_{u,t}^l - \mathbf{w}_{t+1}^l \right) \mid |\mathcal{U}_t^l| = K \right]. \tag{A.8}$$

The value in Eq. (A.6) can be bounded using the Lemma 5 of [6]. That is, when K out of U users are uniformly sampled without replacement, the variance of the scheme compared to full users participation is bounded by:

$$\mathbb{E} \left[\left\| \sum_{u \in \mathcal{U}_t^l} \frac{1}{|\mathcal{U}_t^l|} \mathbf{w}_{u,t}^l - \mathbf{w}_{t+1}^l \right\|^2 \mid |\mathcal{U}_t^l| = K \right] \leq \frac{U}{K(U-1)} \left(1 - \frac{K}{U} \right) 4\eta_t^2 G^2.$$

The value in Eq. (A.7) is bounded using the results from Eq. (A.5), thus:

$$p_l^2 \mathbb{E} \left[\|\tilde{\mathbf{w}}_t^l - \mathbf{w}_{t+1}^l\|^2 \right] \leq p_l^2 (v_t^l + \eta_t^2 G^2).$$

Finally, using the result for the mean of K user's update uniformly sampled without replacement in Eq. (A.3), the value in Eq. (A.8) is equal to 0. Adding the three expressions together, we get:

$$\mathbb{E} \left[\|\tilde{\mathbf{w}}_{t+1}^l - \mathbf{w}_{t+1}^l\|^2 \mid |\mathcal{U}_t^l| = K \right] \leq \frac{1}{(1-p_l)^2} \left(p_l^2 (\eta_t^2 G^2 + v_t^l) + \frac{U}{K(U-1)} \left(1 - \frac{K}{U} \right) 4\eta_t^2 G^2 \right). \tag{A.9}$$

Plugging Eq. (A.5) and Eq. (A.9) into Eq. (A.4), we obtain:

$$\begin{aligned}
v_{t+1}^l &= \mathbb{E} \left[\|\tilde{\mathbf{w}}_{t+1}^l - \mathbf{w}_{t+1}^l\|^2 \right] \leq P \left[|\mathcal{U}_t^l| = 0 \right] (v_t^l + \eta_t^2 G^2) \\
&\quad + \sum_{K=1}^U P \left[|\mathcal{U}_t^l| = K \right] \frac{1}{(1-p_l)^2} \left(p_l^2 (\eta_t^2 G^2 + v_t^l) + \frac{U}{K(U-1)} \left(1 - \frac{K}{U} \right) 4\eta_t^2 G^2 \right) \\
&\leq p_l (v_t^l + \eta_t^2 G^2) + \frac{1}{(1-p_l)^2} \left(p_l^2 (\eta_t^2 G^2 + v_t^l) + \frac{4\eta_t^2 G^2 U}{U-1} \right) \sum_{K=1}^U P \left[|\mathcal{U}_t^l| = K \right] \\
&= p_l (v_t^l + \eta_t^2 G^2) + \frac{1}{1-p_l} \left(p_l^2 (\eta_t^2 G^2 + v_t^l) + \frac{4\eta_t^2 G^2 U}{U-1} \right) \\
&= \frac{p_l}{1-p_l} v_t^l + \eta_t^2 G^2 \left(\frac{\frac{4U}{U-1} + p_l}{1-p_l} \right).
\end{aligned}$$

This yields a recursive upper bound on the per-layer update variance v_{t+1}^l as a function of the previous round's variance v_t^l :

$$v_{t+1}^l \leq D \cdot v_t^l + E, \quad v_1^l = 0, \quad (\text{A.10})$$

where

$$D \triangleq \frac{p_l}{1-p_l} \quad \text{and} \quad E \triangleq \eta_t^2 G^2 \left(\frac{\frac{4U}{U-1} + p_l}{1-p_l} \right). \quad (\text{A.11})$$

Since $p_l \leq p_1 < 0.5$, it follows that $D = \frac{p_l}{1-p_l} < 1$, ensuring that the recurrence is contractive and thus leads to convergence of the variance sequence:

$$v_{t+1}^l \leq D \cdot v_t^l + E \leq D^2 v_{t-1}^l + E + DE \stackrel{(a)}{\leq} E \sum_{k=0}^{t-1} D^k + \underbrace{D^t v_1^l}_0 = \frac{1-D^t}{1-D} E,$$

where (a) follows since Eq. (A.10).

Substituting D and E given in Eq. (A.11), we have:

$$v_{t+1}^l \triangleq \sum_{l=1}^L \mathbb{E} \left[\|\tilde{\mathbf{w}}_{t+1}^l - \mathbf{w}_{t+1}^l\|^2 \right] \leq \frac{1-D^t}{1-D} E \leq \frac{E}{1-D} = \eta_t^2 G^2 \left(\frac{\frac{4U}{U-1} + p_l}{1-2p_l} \right).$$

Now, summing over the L layers:

$$\begin{aligned}
\mathbb{E} \left[\|\tilde{\mathbf{w}}_{t+1} - \mathbf{w}_{t+1}\|^2 \right] &= \sum_{l=1}^L \mathbb{E} \left[\|\tilde{\mathbf{w}}_{t+1}^l - \mathbf{w}_{t+1}^l\|^2 \right] \\
&\leq \sum_{l=1}^L \eta_t^2 G^2 \left(\frac{\frac{4U}{U-1} + p_l}{1-2p_l} \right) \leq \eta_t^2 G^2 \frac{4U}{U-1} \sum_{l=1}^L \frac{1+p_l}{1-2p_l}.
\end{aligned}$$

Substituting p_l , as given in Lemma 1, with the value in Lemma 1 gives:

$$\mathbb{E} \left[\|\tilde{\mathbf{w}}_{t+1} - \mathbf{w}_{t+1}\|^2 \right] \leq \eta_t^2 G^2 \frac{4U}{(U-1)} \sum_{l=1}^L \frac{1+Q \left(L+1-l, \frac{T_t^d}{m} \right)^U}{1-2Q \left(L+1-l, \frac{T_t^d}{m} \right)^U},$$

thus proving Lemma 3. \square

A.4 Appendix D - Proof of Theorem 1

We start by using the full participation FedAvg update \mathbf{w}_{t+1} :

$$\begin{aligned}
\mathbb{E} \left[\|\tilde{\mathbf{w}}_{t+1} - \mathbf{w}_{opt}\|^2 \right] &= \mathbb{E} \left[\|\tilde{\mathbf{w}}_{t+1} - \mathbf{w}_{t+1} + \mathbf{w}_{t+1} - \mathbf{w}_{opt}\|^2 \right] \\
&= \underbrace{\mathbb{E} \left[\|\tilde{\mathbf{w}}_{t+1} - \mathbf{w}_{t+1}\|^2 \right]}_{S_1} + \underbrace{\mathbb{E} \left[\|\mathbf{w}_{t+1} - \mathbf{w}_{opt}\|^2 \right]}_{S_2} + \underbrace{2 \langle \tilde{\mathbf{w}}_{t+1} - \mathbf{w}_{t+1}, \mathbf{w}_{t+1} - \mathbf{w}_{opt} \rangle}_{S_3}.
\end{aligned}$$

We note that S_3 vanishes by the unbiasedness Lemma 2. S_1 is bounded using Lemma 3:

$$\mathbb{E} \left[\|\tilde{\mathbf{w}}_{t+1} - \mathbf{w}_{t+1}\|^2 \right] \leq \eta_t^2 G^2 \frac{4U}{(U-1)} \sum_{l=1}^L \frac{1 + Q \left(L+1-l, \frac{T_t^d}{m} \right)^U}{1 - 2Q \left(L+1-l, \frac{T_t^d}{m} \right)^U}.$$

The term S_2 is bounded using Lemma 1 from [6], which states that under Assumption A1 and a step size satisfying $\eta_t \leq \frac{1}{4L}$, the following inequality holds:

$$\mathbb{E} \left[\|\tilde{\mathbf{w}}_{t+1}^l - \mathbf{w}_{opt}\|^2 \right] = (1 - \eta_t \rho_c) \mathbb{E} \left[\|\tilde{\mathbf{w}}_t^l - \mathbf{w}_{opt}\|^2 \right] + \underbrace{\eta_t^2 \mathbb{E} \left[\|g_t - \bar{g}_t\|^2 \right]}_{\tilde{F}} + 6\eta_t^2 \rho_s \Gamma, \quad (\text{A.12})$$

where g_t and \bar{g}_t are defined by:

$$g_t \triangleq \frac{1}{U} \sum_{u=1}^U \nabla F_u(\mathbf{w}; i_t^u) \quad \bar{g}_t \triangleq \frac{1}{U} \sum_{u=1}^U \nabla F_u(\mathbf{w}).$$

The quantity \tilde{F} in Eq. (A.12) corresponding to the variance of the stochastic gradient error, admits the following upper bound:

$$\begin{aligned} \eta_t^2 \mathbb{E} \left[\|g_t - \bar{g}_t\|^2 \right] &= \eta_t^2 \mathbb{E} \left\| \sum_{u=1}^U \frac{1}{U} (F_u(\mathbf{w}; i_t^u) - \nabla F_u(\mathbf{w})) \right\|^2 \\ &= \eta_t^2 \frac{1}{U^2} \sum_{u=1}^U \mathbb{E} \left\| (F_u(\mathbf{w}; i_t^u) - \nabla F_u(\mathbf{w})) \right\|^2 \\ &\leq \eta_t^2 \frac{1}{mU^2} \sum_{u=1}^U \frac{\sigma_u^2}{P_u}, \end{aligned}$$

where the last inequality stems from Assumption A2.

Combining the bounds for S_1 and S_2 , we obtain:

$$\mathbb{E} \left[\|\tilde{\mathbf{w}}_{t+1} - \mathbf{w}_{opt}\|^2 \right] \leq (1 - \eta_t \rho_c) \mathbb{E} \left[\|\tilde{\mathbf{w}}_t - \mathbf{w}_{opt}\|^2 \right] + \eta_t^2 (B + C_t),$$

where B and C_t are given by:

$$B \triangleq \frac{1}{mU^2} \sum_{u=1}^U \frac{\sigma_u^2}{P_u} + 6\rho_s \Gamma \quad C_t \triangleq G^2 \frac{4U}{U-1} \sum_{l=1}^L \frac{1 + Q \left(L+1-l, \frac{T_t^d}{m} \right)^U}{1 - 2Q \left(L+1-l, \frac{T_t^d}{m} \right)^U}.$$

By repeatedly applying the recursive relation from the final model \mathbf{w}_{R+1} , we obtain:

$$\mathbb{E} \left[\|\tilde{\mathbf{w}}_{R+1} - \mathbf{w}_{opt}\|^2 \right] \leq \prod_{t=1}^R (1 - \eta_t \rho_c) \Delta_1 + \sum_{t=1}^R \eta_t^2 (B + C_t) \prod_{\tau=t+1}^R (1 - \eta_\tau \rho_c),$$

where $\Delta_1 \triangleq \mathbb{E} \left[\|\tilde{\mathbf{w}}_1 - \mathbf{w}_{opt}\|^2 \right]$, thus proving Theorem 1. \square